JOURNAL OF CATALYSIS 151, 87–95 (1995)

ESR Studies of Well-Dispersed Ag Crystallites on SiO_2

Xiangmin Li and Albert Vannice

Department of Chemical Engineering, Pennsylvania State University, University Park, Pennsylvania 16802-4400

Received July 13, 1994; revised September 7, 1994

ESR was utilized to study Ag on SiO_2 over a dispersion range of 0.04 to 0.32, which gave average Ag crystallites sizes between 4 and 31 nm. For all samples only a single sharp signal was observed at $g = 2.0028 \pm 0.0002$ with a peak-to-peak linewidth of 1.5–6.0 G, whether after reduction at 773 K or after adsorption of O_2, N_2O or C_2H_5Cl. This signal was shown to be associated with conduction electrons existing only in small nanocrystallites (ca. 7 nm or smaller) in which quantum size effects occur to increase the spin relaxation time and provide a CESR signal. The use of ^{17}O verified the peak was not due to any paramagnetic oxygen species. No correlation between line width or g shift and average crystallite size (below 7 nm) was observed, although a model invoking quantum size effects has predicted one. Adsorption of O_2 or N_2O at either 300 or 443 K produced identical results—the peak intensity was decreased and no new peaks were detected. Exposure to H_2 at 443 or 300 K provided almost complete or partial restoration of the signal, respectively. Adsorption of C_2H_5Cl at 300 K had no effect, but at 523 K adsorption on clean Ag markedly decreased intensity, and adsorption on an oxygen-covered Ag surface further decreased signal strength, thus indicating the strong interaction Cl atoms can achieve when such promoters are used in the partial oxidation of ethylene.

INTRODUCTION

Silver plays a unique role in partial oxidation reactions as it is the only metal with sufficiently high selectivity to allow its use in commercial processes to produce ethylene oxide. Silver is also used to obtain formaldehyde from methanol. For highest yields, commercial silver catalysts utilize α-Al_2O_3 and are very poorly dispersed (1–4); however, well-dispersed Ag on SiO_2 can also provide surprisingly high selectivity to ethylene oxide (5). Many studies have been conducted to better understand the state of the Ag surface under reaction conditions, the role of Cl-containing promoters, and the oxygen species involved (1–4); the general consensus currently is that the reactants adsorb on an oxidized Ag surface modified by Cl, and atomic oxygen is the principal oxygen species involved in both ethylene oxide and CO_2 formation (4). Additional information about the interaction of oxygen and a Cl-containing promoter with Ag as well as the influence of Ag crystallite size on electronic and adsorption properties would therefore be of some interest. Furthermore, silver catalysts are more difficult to characterize than most noble-metal catalysts because Ag chemisorbs few gases, and although oxygen is one that does chemisorb, the possibility of subsurface oxygen formation complicates analyses (6). When Ag crystallites become too small, X-ray diffraction (XRD) peaks become too broad to be distinguished from the support and resolution between Ag particles and the support material by TEM becomes difficult. Thus a technique sensitive to very small Ag crystallites would be useful.

For these reasons, a family of Ag/SiO_2 catalysts with a wide range of dispersion was characterized by CESR (conduction electron spin resonance) as well as O_2 chemisorption, XRD, and TEM. ESR spectra were obtained for these Ag catalysts after reduction in H_2, after O_2 and N_2O chemisorption, and after adsorption of C_2H_5Cl on both clean and O-covered Ag surfaces. A model by Kawabata predicts a correlation between the square of the particle diameter and the CESR linewidth for particles small enough to be affected by quantum size effects (ca. 7 nm or less for Ag at 300 K) (7); consequently, we wanted to determine if this approach might provide another means to estimate dispersion for very small metallic Ag particles. Our results are presented here.

EXPERIMENTAL

Seven different silica-supported silver catalysts were studied: 0.18% Ag/SiO_2, 0.45% Ag/SiO_2, 0.61% Ag/SiO_2, 1.06% Ag/SiO_2, 1.50% Ag/SiO_2, 2.78% Ag/SiO_2, and 16.65% Ag/SiO_2. They varied in silver loading, precursor salt, preparation technique, and average Ag particle size, as listed in Table 1. The silica gel support (Davison, grade 57, 220 m^2/g) was ground and then heated at 823 K for 2 h in air (Linde, dry grade) at a flow rate of 1 ft^3 (STP)/h in order to remove any organic impurities before Ag deposition. The two preparation techniques used—incipient wetness and ion-exchange—have been described previously (8). Each catalyst was dried in an oven overnight at 380 K then transferred into a vial and stored

0021-9517/95 $6.00

TABLE 1

Properties of Ag/SiO_2 Samples after Reduction at 773 K

Ag Loading (wt%)	Gas uptake (μmol/g cat.) O_{2Irr}	H_{2Titr}	Dispersion O_{ad}/Ag_{total}	Ag particle size (nm)
0.18	2.3	4.2	0.28	4.9
0.45	4.6	7.8	0.22	6.1
0.61	8.9	18.7	0.32	4.3
1.06[a,b]	8.0	14.1	0.16	8.2
1.06 sintered[a,b]	3.7	5.5	0.075	18
1.50	12.9	29.8	0.19	7.2
2.78	19.9	41.7	0.15	8.7
16.65[b]	34.2	74.3	0.044	31

[a] Prepared with Ag lactate rather than $AgNO_3$.
[b] Prepared using incipient wetness rather than ion exchange.

in a desiccator. The silver loadings were determined by plasma emission spectroscopy at the Mineral Constitution Laboratory of The Pennsylvania State University except for the 0.61% Ag/SiO_2, 1.06% Ag/SiO_2, and 16.65% Ag/SiO_2 catalysts, which were previously analyzed (5). Oxygen chemisorption and hydrogen titration measurements were performed with a UHV gas adsorption system utilizing a turbomolecular pump (Balzers, TSU 172) which gives a vacuum of 1×10^{-7} Torr in the sample cell, a Baratron pressure gage (MKS, model 310), and a Theall Engineering TP 2200 temperature programmer/controller (9). The gases used for pretreatment and adsorption measurements were O_2 (99.999%, MG Sci.), H_2 (99.999%, MG Sci.), and He (99.999%, Linde). These three gases were ultrahigh purity and further purified by passing them through molecular sieve traps and Oxytraps (Alltech Corp.) except for O_2, which was passed only through the molecular sieve trap. The N_2O (Airco, 99.995%), C_2H_5Cl (MG Sci., CP grade, 99.7% min), and $^{17}O_2$ (Isotec Inc., 11.7 atom% ^{17}O) were used as received.

The sample pretreatment prior to chemisorption or ESR measurements consisted of calcination in 10% O_2, 90% He (40 cm^3 (STP)/min) at 773 K for 2 h, evacuation at 773 K for 20 min, H_2 reduction (20 cm^3 (STP)/min) at 773 K for 2.5 h, and evacuation at 773 K for 20 min (8). One sample of 1.06% Ag/SiO_2 was sintered by heating in air at 800 K for 30 min. The adsorption measurements were conducted at either 443 or 300 K because 443 K optimizes oxygen adsorption on silver to determine dispersion (8, 10). The isotherms at 300 K provided oxygen uptakes for the O_2 ESR experiments conducted at this temperature. The H_2 titration technique was also used at each temperature (6). Typical experimental procedures are described elsewhere (8, 11). The dispersion and average crystallite size of silver were calculated by assuming a stoichiometry of unity for the O_{ad}/Ag_s ratio at 443 K and a surface site density of 1.31×10^{15} Ag_s cm^{-2} (1).

XRD measurements were made using a Rigaku Geigerflex DMAXB X-ray diffractometer with Cu$K\alpha$ radiation and operation at 40 kV, 20 mA with a 2° slit width, and 4°/min. Scans were also carried out on the pure SiO_2 support to establish a background diffraction pattern. When Ag peaks were detected, the sample was rescanned at 0.5°/min for greater sensitivity, and average crystallite sizes were calculated using the Scherrer equation

$$d = \frac{0.89\lambda}{B \cos \theta}, \qquad [1]$$

with Warren's correction ($B = B_M^2 - B_I^2)^{1/2}$, where B_M is the measured linewidth and B_I is the instrumental broadening of 0.12°.

TEM micrographs were obtained for the 0.61% Ag/SiO_2 and 1.06% Ag/SiO_2 samples, which were the most thoroughly studied, with a Philips 420 STEM system operating in the TEM mode at 120 kV. The TEM samples were placed in an acetone slurry in an ultrasonic bath for 30 min, a 400 mesh, carbon-coated copper grid was immersed into the slurry, and the grid was then dried under a heat lamp for 20 min. EDS was used to verify that the particles counted were Ag.

ESR measurements were performed with an IBM (i.e., Bruker) ER 200D-SRC spectrometer using a rectangular TE102 cavity. The sample (~0.3 g) was contained in a 4 mm O.D. quartz ESR tube (Wilmad, 707-SQ) attached to a high-vacuum stopcock (Ace Glass), which allowed *in situ* evacuation, pretreatment, and adsorption of various gases. Approximately 7.5 cm of the quartz tube was filled with the Ag/SiO_2 sample, which was considerably longer

TABLE 2

Chemisorption on Ag/SiO_2 Catalysts at 300 K after Reduction at 773 K

Ag loading (wt%)	Gas uptake (μmol/g cat.) O_{2irr}	H_{2Titr}	Oxygen coverage at 300 K, θ^a
0.18	1.5	2.3	0.65
0.45	2.5	5.2	0.54
0.61	4.0	8.4	0.45
1.06	4.7	9.5	0.59
1.06 sintered	2.0	3.2	0.54
1.50	5.1	10.8	0.40
2.78	8.2	18.1	0.41
16.65	18.9	34.7	0.55

[a] O_{2Irr} (300 K)/O_{2Irr} (443 K). θ_{ave} = 0.52.

TABLE 3

Ag Surface- and Volume-weighted Crystallite Sizes on SiO_2 Calculated from Chemisorption, XRD, and TEM

Ag loading (wt%)	$\bar{d}_{surf}$ (nm) Chem.	TEM	$\bar{d}_{vol}$ (nm) XRD	TEM
0.61	4.3	14.3	7.3	17.7
1.06	8.2	17.8	5.0	22.3
1.06 sintered	17.9	—	9.8	—
1.50	7.2	—	7.8	—
2.78	8.7	—	8.3	—
16.65	30.5	—	20.4	—

than the ESR cavity dimension, to avoid any effect due to change in the sample position inside the cavity. After pretreatment on the UHV adsorption system, the cell was moved to the ESR cavity and reconnected to the system via 6.4 mm copper tubing, which allowed gases to be introduced and evacuated without moving the cell (12). The ESR baseline for the empty cell in the cavity was recorded first and then subtracted from each Ag/SiO_2 ESR spectrum using a computer. A weak pitch standard (3.3 ppm in KCl) was used to establish g values and known peak areas and allow spin densities to be determined. Details are given elsewhere (11).

RESULTS

O_2 chemisorption and H_2 titration uptakes at 443 K are listed in Table 1 along with dispersions and crystallite sizes based on O coverages. A similar set of results obtained at 300 K is provided in Table 2. The fraction of the Ag surface covered by oxygen during the ESR measurments at 300 K can be estimated by the ratio of the O_2 uptakes listed in Tables 1 and 2, and the average coverage at 300 K is approximately constant and close to one-half (θ_{ave} = 0.52). Particle size distributions are shown in Fig. 1 for the two samples characterized by TEM, and the surface-weighted and volume-weighted particle sizes calculated from these results, $\bar{d}_{surf}$ and $\bar{d}_{vol}$, respectively, are listed in Table 3.

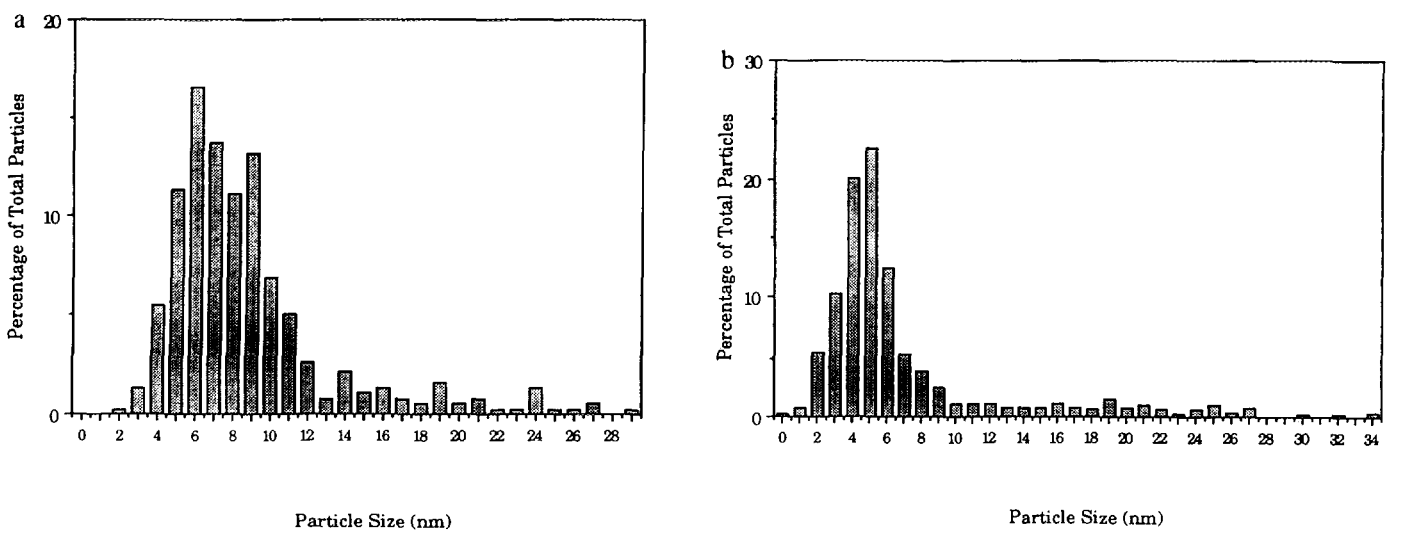

FIG. 1. (a) Particle size distribution for 0.61% Ag/SiO_2 (380 particles counted via TEM), (b) particle size distribution for 1.06% Ag/SiO_2 (507 particles counted via TEM).

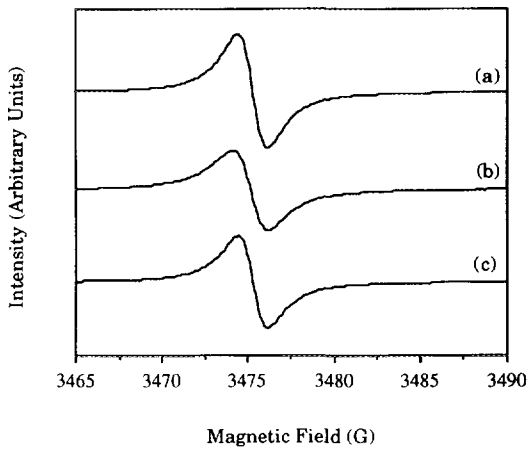

FIG. 2. CESR spectra for 0.61% Ag/SiO_2: (a) after reduction at 773 K for 2 h and cooling to 300 K, (b) after O_2 adsorption at 20 Torr and 300 K for 30 min and evacuation at 300 K for 30 min, (c) after H_2 titration at 45 Torr and 300 K for 30 min and evacuation at 300 K for 30 min.

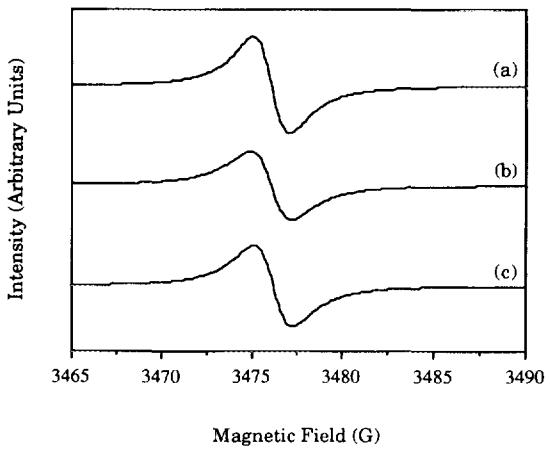

FIG. 3. CESR spectra for 1.06% Ag/SiO_2: (a) after reduction at 773 K for 2 h and cooling to 300 K, (b) after O_2 adsorption at 20 Torr and 300 K for 30 min and evacuation at 300 K for 30 min, (c) after H_2 titration at 45 Torr and 300 K for 30 min and evacuation at 300 K for 30 min.

CESR spectra after reduction in H_2 and after O_2 adsorption for the two most thoroughly studied catalysts—0.61% Ag/SiO_2 and 1.06% Ag/SiO_2—are shown in Figs. 2 and 3. They are representative of all these SiO_2-supported Ag samples (11). A pure SiO_2 support gave no signal. All ESR line-shapes were symmetric with a g value of 2.0028 ± 0.0002 and peak-to-peak (ΔH_{pp}) linewidths varying only between 1.5–6.0 G. The spin densities were determined before and after O_2 adsorption by double integration of the derivative ESR signal and comparison to the weak pitch sample, and these values are listed in Table 4. The presence of gas-phase O_2 allowed weak oxygen adsorption to occur which caused noticeable broadening of the signals. After exposure to oxygen, no new ESR signals were ever detected but the intensity of the peak at 2.0028 invariably was decreased compared to the clean sample. O_2 adsorption at 443 K, rather than 300 K, produced similar results, i.e., no new ESR signals and a decreased signal intensity (11). One set of experiments with $^{17}O_2$-enriched oxygen (12%) produced identical results with no hyperfine structure, which would occur if the signal at $g = 2.0028$ were due to O^- or O_2^- species. Titration of some of the absorbed oxygen by H_2 occurred even at 300 K, as demonstrated by both the measured uptakes and the partial restoration of the ESR signals in Figs. 2 and 3.

Adsorption of N_2O on these Ag/SiO_2 samples at either 300 or 443 K generated ESR spectra essentially identical to those obtained after O_2 adsorption, as shown in Fig. 4. N_2O is known to dissociatively chemisorb on Ag giving only atomic oxygen (2, 4). The signal again increased after exposure to H_2 at 300 K (11).

Several Ag/SiO_2 samples were exposed to C_2H_5Cl, and ESR spectra were obtained after C_2H_5Cl adsorption at 300 and 523 K on a clean, reduced Ag surface and after adsorption at 523 K on an O-covered Ag surface (following oxygen chemisorption at 443 K). Results for 1.06% Ag/SiO_2 are shown in Fig. 5. Although adsorption oc-

TABLE 4

Fractional Spin Density Decrease after O_2 Adsorption at 300 K

Ag loading (wt%)	Spin density after reduction at 773 K (spin/g cat × 10^{-15})	Spin density after O_2 adsorption at 300 K (spin/g cat × 10^{-15})	Fractional spin density decrease
0.18	1.96	1.65	0.16
0.45	0.37	0.31	0.16
0.61	2.65	2.29	0.14
1.06	10.86	10.08	0.07
1.06 sintered	1.68	1.54	0.08
1.50	0.23	0.18	0.22
2.78	3.51	3.00	0.15
16.65	very small	—	—

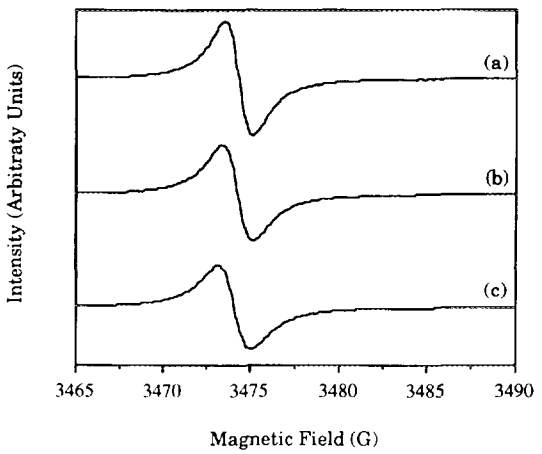

FIG. 4. CESR spectra for 0.61% Ag/SiO_2: (a) after reduction at 773 K for 2 h and cooling to 300 K, (b) after N_2O adsorption at 20 Torr and 300 K for 30 min and evacuation at 300 K for 30 min, (c) after additional N_2O adsorption at 20 Torr and 443 K for 3 h and evacuation at 443 K for 30 min and cooling to 300 K.

curred at 300 K, essentially no change was observed in the ESR signal thus implying only weak physisorption existed (11). In contrast, adsorption at 523 K decreased the ESR signal considerably, even after evacuation, implying that C_2H_5Cl chemisorption, presumably dissociative, had occurred (Fig. 5A). O_2 adsorption at 443 K on clean Ag decreased the signal, as stated earlier, but C_2H_5Cl adsorption on this O-covered surface produced an additional decrease in signal intensity, as indicated in Fig. 5B, thus providing direct evidence that Cl-containing organic promoters can adsorb strongly on either clean or O-covered Ag surfaces. Again all line shapes remained symmetric with $g = 2.0028 \pm 0.0002$ and $\Delta H_{pp} = 1.5$–6.0 G.

DISCUSSION

Electron spin resonance (ESR) has been used previously to characterize small Ag clusters and crystallites as well as oxygen species adsorbed on these surfaces (13–29); however, only three studies have addressed SiO_2-supported Ag (21–23). Four types of paramagnetic species have been proposed to exist in these O_2/Ag systems: unpaired electrons in Small Ag clusters with a positive charge, $Ag_x^{\delta+}$, where $(x - \delta)$ is an odd number and x is typically ≤ 10; conduction electrons in Ag nanocrystallites, bulk-like conduction electrons in large Ag crystallites, and O_2^- or O^- absorbed on the Ag surface. Our interest in applying conduction electron spin resonance (CESR) to this family of dispersed Ag particles covering a range of crystallite size was threefold: to examine the effect of chemisorbed oxygen, N_2O and C_2H_5Cl on the conduction electrons via the CESR signal, to determine if the quantum size effects relating crystalline size and peak width proposed by Kawakata (7) could allow measurement of small Ag particles, and to see if any paramagnetic oxygen species were formed on these Ag surfaces after chemisorption.

A. Identification of Paramagnetic Species

Very small Ag particles (ca. 1–3 nm) have been prepared in vacuum by condensing Ag atoms into inert matrices at low temperatures and have been studied by Monot and co-workers (13–15) and by Ozin (16). In addition to two hyperfine-split spectra associated with iso-

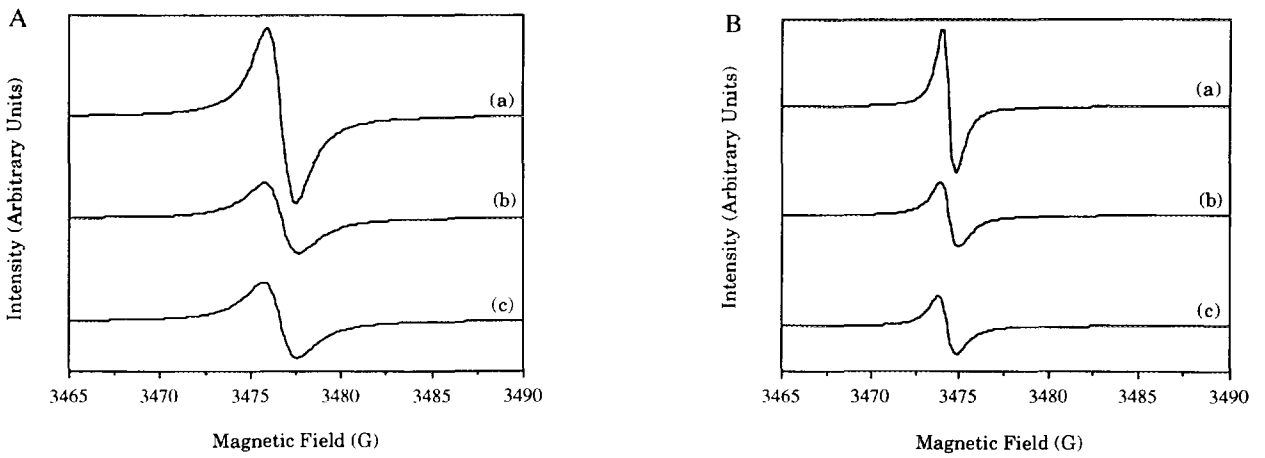

FIG. 5(A) CESR Spectra for 1.06% Ag/SiO_2: (a) after reduction at 773 K for 2 h and cooling to 300 K, (b) in the presence of 20 Torr C_2H_5Cl after exposure at 523 K for 1 h and cooling to 300 K, (c) after evacuation of C_2H_5Cl at 300 K for 30 min. (B) CESR Spectra for 1.06% Ag/SiO_2: (a) after reduction at 773 K for 2 h and cooling to 300 K, (b) after O_2 adsorption at 20 Torr and 443 K for 30 min, evacuation at 443 K for 30 min, and cooling to 300 K, (c) after C_2H_5Cl adsorption at 20 Torr and 523 K for 1 h, evacuation at 523 K for 30 min, and cooling to 300 K.

lated ^{107}Ag and ^{109}Ag atoms, Monot *et al.* obtained a narrow (ΔH_{pp} = 15–20 G) signal between g = 2.007 and 2.016 which was attributed to conduction electrons in small Ag particles and had a Curie-type dependence; i.e., the intensity increased as temperature decreased (13–15). Ozin also obtained ESR signals for isolated Ag atoms in addition to a narrow CESR signal between g values of 2.013 to 2.028 (16). For larger, 5–30 nm colloidal Ag particles, a narrow (ΔH_{pp} = 10–14 G) CESR signal at g = 2.034 was reported by Jain *et al.* (17). Silver-exchanged zeolites have been reduced and studied by three different groups. Hyperfine-split spectra as well as other signals were observed in all three cases. The former signal, reported at a g value of 2.053, 2.025, and 1.973 by Hermerschmidt and Haul (18), Grobet and Schoonheydt (19), and Xu and Kevan (20), respectively, was associated with $Ag_x^{\delta+}$ clusters, while the latter signals with g values of 1.909 (18), 1.981 (19), and 1.950–2.004 (20) were attributed to conduction electrons in small Ag particles both within the super cages and on the external surface. Linewidths of these signals varied from 6 to 135 G. Sintering of the Ag led to a loss of the CESR signal (18). For somewhat larger Ag crystallites on SiO_2, g values (and linewidths) of 2.002 (6 G), 2.001 (17 G), and 1.980 (175 G) have been reported by Gravelle and co-workers (21), Wang *et al.* (22), and Shimizu *et al.* (23), respectively. No CESR signal was observed with a Ag/TiO_2 sample reduced at 473 K (24).

After exposure of Ag to O_2, asymmetric ESR spectra have been obtained for adsorbed oxygen due to its anisotropic environment at the surface, and in all cases the signal has been assigned to an O_2^- species. Clarkson and co-workers observed only such spectra for O_2^- on Vycor-supported Ag (25–27), while Hermerschmidt and Haul reported such spectra for O_2^- on Ag/zeolites along with a CESR signal after reduction at various temperatures (28). Shimizu *et al.* also reported an O_2^- spectrum for a Ag/SiO_2 sample (23), and only an O_2^- spectrum was obtained after O_2 adsorption on unsupported AgO (29).

For all the Ag/SiO_2 samples in this study, a single, narrow symmetric signal at 2.0028 ± 0.0002 was obtained regardless of pretreatment or adsorbate; the only significant variation was in signal intensity. Based on the preceding discussion, this signal is definitely not due to a paramagnetic oxygen species. This was confirmed by chemisorbing $^{17}O_2$-enriched oxygen on the 0.61% Ag/SiO_2 catalyst and obtaining the ESR spectrum—no hyperfine splitting was observed and the spectrum was essentially identical to that obtained with $^{16}O_2$ (11). The assignment of this ESR signal to very small Ag clusters ($Ag_x^{\delta+}$) can also be disallowed because no hyperfine splitting was ever observed, as expected for these clusters (18–20). Thus it is clearly a CESR signal; the question is whether it represents conduction electrons in large, bulk-like Ag crystallites or electrons in much smaller Ag nanocrystallites.

B. Crystallite Size Effects on CESR in Metals

Few reports exist of CESR in bulk metals because relaxation mechanisms are extremely efficient and relaxation times are very short, which results in extremely broad signals even at 77 K, although some spectra have been obtained near 4 K (7, 30). Only the unpaired electrons near the top of the Fermi distribution in a metal can contribute to the CESR signal; this fraction of the total number of electrons, k_BT/E_F, when multiplied by the total electron density, $N\beta^2/k_BT$, gives the well-known, temperature-independent, Pauli-type paramagnetic susceptibility, $N\beta^2/E_F$, where N is the number of atoms per volume, β is the Bohr magneton, k_B is Boltzmann's constant, and E_F is the Fermi energy level (31). A theory of CESR line shapes for bulk metals was worked out by Dyson (32) and confirmed experimentally by Kip *et al.* (33, 34). Schultz *et al.* have reported a g value of 1.983 for bulk silver between 2 and 18 K (35), which was later confirmed by Nishida and Horai (36). The CESR signals obtained in this study are approximately two orders of magnitude narrower than those expected for heavy Group IB bulk metals and must be associated only with conduction electrons in Ag nanocrystallites.

The spin relaxation time, τ, for conduction electrons in bulk metals is dominated by spin–orbit coupling and is approximately related to the resistivity scattering time, τ_R, as $\tau = \tau_R/C$ where C depends on the square of the g shift of the metal (37). This must be modified when the metal crystallites become small enough so that surface scattering effects must be considered, that is, when the diameter, d, approaches the mean free path of the electron (7). The relaxation time is then $1/\tau = C(1/\tau_R + 2V_F/d)$ where V_F is the Fermi velocity. Furthermore, when the crystallites become sufficiently small so that the average energy spacing, δ, becomes larger than the Zeeman (spin–flip) energy W_z, i.e., $\hbar W_z/\delta \ll 1$, and the spin–orbit coupling is not strong, i.e., $\hbar/\tau\delta \ll 1$, where $\hbar$ is $1/2\pi$ h (Planck's constant), Kawabata has shown that these quantum size effects produce a quenching effect on the relaxation processes, thus increasing the relaxation time (7)

$$\frac{1}{\tau} = C\left(\frac{1}{\tau_R} + \frac{2V_F}{d}\right)\left(\frac{\hbar W_z}{\delta}\right). \qquad [2]$$

Kubo had previously shown that quantum size effects would alter the electronic properties of sufficiently small metal particles and that $\delta = 4E_F/3N'$ where N' is the number of atoms in the particle (30). Consequently, this model for small metal crystallites predicts that as the

quantum limits are attained, i.e., $\hbar W_z/\delta \ll 1$ and $\hbar/\tau\delta \ll 1$, a new, narrow CESR peak will grow out of the broad background (7). At 300 K, using a Fermi energy of 5.48 eV for Ag, this regime for Ag should be attained at a crystallite size of approximately 6–8 nm or less (11, 14).

Kawabata has derived correlations for these small particles indicating that both the linewidth, ΔH_{pp}, and the g shift are approximately equal to $\hbar W_z/\pi\delta$ (7); therefore, using the g shift of -0.019 for bulk Ag (35), our experimental resonance frequency of $f = 9.77 \pm 0.01$ GHz, and our observed g value of 2.0028 ± 0.0002, it can be shown that the equations derived by Kawabata simplify to

$$d^2(\text{Å}) = 3.30\ \Delta H_{pp}\ (\text{G}) \qquad [3]$$

or

$$d^2(\text{Å}) = -3.30\ (g\ \text{shift})(\text{G}), \qquad [4]$$

where the g shift is the g value for the small particles minus that for bulk Ag (11).

The symmetry and linewidths of the CESR spectra obtained in this study are completely consistent with that anticipated from Kawabata's model, and these spectra are similar to those associated previously with CESR in small Ag particles although our signals are routinely narrower and the g values are typically lower; however, the agreement with the parameters reported by Gravelle *et al.* for 2% Ag/SiO_2 is excellent (21). Despite this consistency, we found no significant variation in crystallite sizes calculated from either Eqs. [3] or [4], as they were routinely around 3 Å based on linewidth and typically near 11 Å based on the g shift (11); furthermore, either set of values is much too small compared to the crystallite sizes listed in Table 3. Consequently, we have found that observed CESR linewidths do not narrow noticeably as the crystallite size decreases below 10 nm, and Kawabata's derivations are not sufficiently refined to allow their use to measure Ag crystallite size.

Additional evidence that the signals observed in these samples are associated with electrons in very small particles is provided by double integration to obtain spin densities. As shown in the second column of Table 4, there is no correlation between spin density and Ag loading (or crystallite size); furthermore, if the density of unpaired conduction electrons in each sample is estimated at 300 K, i.e., that which could be observable by ESR,

$$N_{ob} = N\left(\frac{kT}{E_F}\right), \qquad [5]$$

it is invariably larger by a factor of 25 (for 0.18% Ag/SiO_2) to almost 10^5 (for 16.65% Ag/SiO_2). If, however, the CESR signal is assumed to arise only from electrons in Ag crystallites small enough to induce quantum size effects, i.e., smaller than about 7 nm, a comparison of spin densities can be made for the 0.61% Ag/SiO_2 and 1.06% Ag/SiO_2 samples because the particle size distributions in Fig. 1 can be used to estimate the volume fraction of Ag in this size range. These spin densities, calculated using Eq. [5] based on the total number of conduction electrons in Ag nanocrystallites smaller than 7 nm, are 1.6×10^{16} ESR observable electrons per gram 0.61% Ag/SiO_2, about four times higher than the density in Table 4, whereas the calculated number for 1.06% Ag/SiO_2 is 1.7×10^{16} e^-/g catalyst, which agrees well with the measured value of 1.1×10^{16} e^-/g in Table 4 (11).

C. Effect of Adsorbates on ESR Spectra

The signals attributed to the conduction electrons broaden significantly in the presence of reversibly adsorbed oxygen, but after evacuation the signals at 2.0028 regained their initial linewidth although their intensity was decreased, as shown in Figs. 2 and 3. The obvious conclusion from this behavior is that a fraction of the conduction electrons becomes localized after irreversible oxygen chemisorption occurs—this constitutes about one-half a monolayer at 300 K, as indicated in Table 2. Strong chemisorption of oxygen is known to occur on Ag surfaces, and the heat of adsorption is higher on small crystallites compared to large crystallites and bulk surfaces (38). Consequently, one might anticipate a correlation between the fraction of Ag atoms at the surface and the reduction in signal strength after O_2 adsorption, and one does exist, as shown in Fig. 6. Although there is significant scatter, part of which is undoubtedly due to

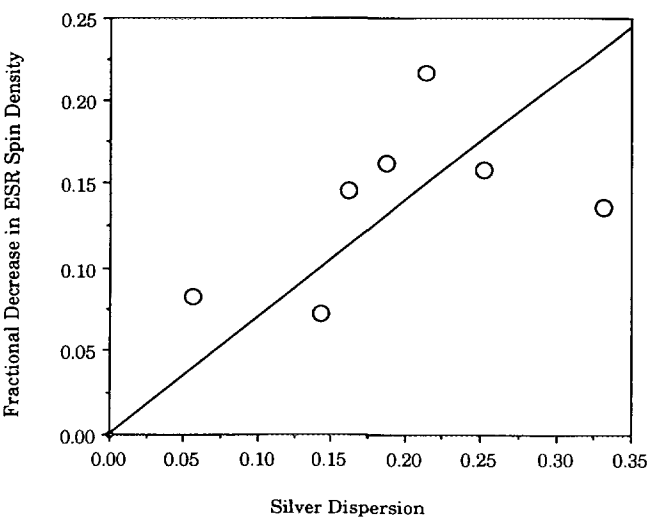

FIG. 6. Correlation of fractional decrease in spin density after O_2 adsorption at 300 K with silver dispersion (based on O_{ad}). The slope is 0.7 ± 0.1 (within 90% probability limits).

the effect of crystallite size distribution on the CESR strength, a clear trend is observable. The only difference between O_2 chemisorption at 300 and 493 K was a greater decrease in CESR signal intensity due to an increase in surface coverage (11). Titration of chemisorbed oxygen by H_2 at 443 K restored signal intensity almost completely while at 300 K partial recovery was obtained, thus indicating that a significant fraction of this oxygen is reactive with H_2 at room temperature (11).

Adsorption of N_2O on Ag is dissociative to give atomic oxygen, and it provides a surface coverage of oxygen at 443 K essentially equal to that obtained during O_2 chemisorption (10, 39). The effect of N_2O adsorption on the CESR signal was consistent with this chemistry, i.e., no paramagnetic oxygen species was formed, adsorption at 300 K reduced the signal intensity, and adsorption at 443 K decreased the CESR signal further, as illustrated in Fig. 4. Hydrogen titration at 300 K again provided partial restoration of the CESR signal intensity (11). This similarity in behavior strongly implies that only nonparamagnetic atomic oxygen exists on these small Ag crystalites, most probably an O^{2-}-type species.

Chlorine-containing hydrocarbons such as ethyl chloride are added to the feed in the ethylene partial oxidation process to promote selectivity to ethylene oxide (1–4). Single-crystal studies have shown that Cl interacts strongly with Ag(111) and Ag(110) surfaces to suppress ethylene combustion; this has been viewed as an electronic effect creating $Ag^{\delta+}$ sites (40–42) although an ensemble effect has also been proposed (41, 42). When C_2H_5Cl was adsorbed at 300 K on a clean reduced Ag/SiO_2 sample, essentially no change was detected in the CESR signal, as mentioned before (11). When, however, the same experiment was conducted at 523 K, the CESR signal intensity decreased by 60%, as demonstrated in Fig. 5A. These results strongly imply only physisorption occurs at 300 K, whereas at reaction temperature chemisorption occurs, presumably dissociative, to allow a strong interaction between Cl atoms and electrons in the Ag crystallites because the decrease observed after C_2H_5Cl adsorption on this catalyst was greater than that obtained after O_2 chemisorption. Our results also show that C_2H_5Cl was adsorbed at 523 K on an oxygen-covered Ag surface; for example, after oxygen chemisorption and evacuation at 443 K, the CESR signal was decreased by 52%, and after heating this sample to 523 K, chemisorbing C_2H_5Cl, and cooling to 300 K, the intensity was further decreased to 61% of its initial value. Figure 5B shows this behavior. This is clear evidence that Cl-containing promoters can effectively adsorb on both clean and O-covered Ag surfaces at typical reaction temperatures, and the pronounced effect of the Cl atoms on the conduction electrons is clear support for the role of Cl as an electronic promoter. This interaction between Cl and O-covered Ag surfaces is consistent with the significant effect that very small concentrations of Cl-containing hydrocarbon promoters have on selectivity to ethylene oxide during ethylene oxidation.

SUMMARY

This family of Ag/SiO_2 catalysts was thoroughly reduced at 773 K after a calcination step and then handled carefully in a UHV system to prevent any exposure to air. This procedure gave metallic Ag particles with a range of dispersion from 0.04 to 0.32, thus providing average crystallite sizes between 4 and 31 nm. Under these conditions, symmetric ESR signals with essentially invariant g values and linewidths were obtained with all samples. The absence of hyperfine splitting eliminated small, positively charged Ag clusters as the source, and the narrow linewidth cannot be associated with conduction electrons in large, bulk-like Ag particles. Adsorption of oxygen produced no new peaks and only diminished the original signal, while adsorption of ^{17}O-enriched oxygen gave no hyperfine splitting; thus no signals attributable to paramagnetic oxygen species were observed. The ESR signals observed in this study would therefore be associated only with conduction electrons in Ag crystallites small enough to be susceptible to quantum size effects which increase the spin relaxation time and narrow the CESR signal, as described by Kubo and Kawabata (7, 30). However, the model derived by the latter author is not sufficiently refined to allow the predicted relationship between crystallite size and linewidth (or g shift) to be observed; consequently, this technique cannot augment other methods to measure the size of very small Ag nanocrystallites.

The adsorption of O_2 or N_2O produced no paramagnetic oxygen species on these Ag crystallites, and the only effect was a decrease in the CESR signal strength that was proportional to the Ag dispersion. From this behavior it is concluded that chemisorbed oxygen atoms strongly interact with the conduction electrons to form essentially surface O^{2-} species. Reaction with H_2 at 443 K restores the signal almost to its original strength, and even at 300 K substantial restoration occurs via this reaction which removes oxygen via water formation.

Adsorption of ethyl chloride on clean Ag had no effect at 300 K but at 523 K it resulted in a marked decrease in the signal intensity, presumably due to dissociative chemisorption allowing Cl atoms to interact with the conduction electrons. At 523 K, ethyl chloride adsorption on an O-covered Ag surface also occurred to further decrease the CESR signal strength, consistent with its capability to act as an electronic promoter during the partial oxidation of ethylene to ethylene oxide.

ACKNOWLEDGMENTS

This research was supported by the NSF under Grant CTS-9019612. Discussions with Professor W. N. Delgass on this topic are also gratefully acknowledged.

REFERENCES

1. Kilty, P. A., and Sachtler, W. M. H., *Catal. Rev.-Sci. Eng.* **10,** 1 (1974).
2. Verykios, X. E., Stein, F. P., and Coughlin, R. W., *Catal. Rev.-Sci. Eng.* **22,** 197 (1980).
3. Sachtler, W. M. H., Backx, C., and van Santen, R. A., *Catal. Rev.-Sci. Eng.* **23,** 127 (1981).
4. van Santen, R. A., and Kuipers, H. P. C. E., *Adv. Catal.* **35,** 265 (1987).
5. Seyedmonir, S. R., Plischke, J. K., Vannice, M. A., and Young, H. W., *J. Catal.* **123,** 534 (1990).
6. Seyedmonir, S. R., Strohmayer, D. E., Geoffroy, G. L., and Vannice, M. A., *J. Catal.* **87,** 424 (1984).
7. Kawataba, A., *J. Phys. Soc. Jpn.* **29,** 902 (1970).
8. Plischke, J. K., and Vannice, M. A., *Appl. Catal.*, **42,** 255 (1988).
9. Chen, A. A., Kaminsky, M., Geoffroy, G. L., and Vannice, M. A., *J. Phys. Chem.* **90,** 4810 (1986).
10. Scholten, J. J. F., Konvalinka, J. A., and Beekman, F. W., *J. Catal.* **28,** 209 (1973).
11. Li, X., M. S. Thesis, The Pennsylvania State University, 1994.
12. Na, B.-K., Kelly, S. L., Walters, A. B., and Vannice, M. A., *Meas. Sci. Technol.* **2,** 770 (1991).
13. Chatelain, A., Millet, J. L., and Monot, R., *J. Appl. Phys.* **47,** 3670 (1976).
14. Monot, R., Narbel, C., and Borel, J. P., *Nuovo Cimento Soc. Ital. Fis.* **19,** 253 (1974).
15. Monot, R., and Millet, J. L., *J. Phys. Suppl. Lett.* **37,** L45 (1976).
16. Ozin, G. A., *J. Am. Chem. Soc.* **102,** 3301 (1980).
17. Jain, S. C., Arora, N. D., and Reddy, T. R., *Phys. Lett.* **54,** 53 (1975).
18. Hermerschmidt, D., and Haul, R., *Ber. Bunsenges. Phys. Chem.* **84,** 902 (1980).
19. Grobet, P. J., and Schoonheydt, R. A., *Surf. Sci.* **156,** 893 (1985).
20. Xu, B., and Kevan, L., *J. Phys. Chem.* **95,** 1147 (1991).
21. Abou-Kais, A., Jarjoui, M., Vedrine, J. C., and Gravelle, P. C., *J. Catal.* **47,** 399 (1977).
22. Wang, Y.-P., Yeh, C., and Chien, S.-H., *J. Chem. Soc., Faraday Trans. 1* **85,** 2199 (1989).
23. Shimizu, N., Shimokoshi, K., and Yasumori, I., *Bull. Chem. Soc. Jpn.* **46** 2929 (1973).
24. Gonzalez-Elipe, A. R., Soria, J., and Munuera, G., *J. Catal.* **76,** 254 (1982).
25. Clarkson, R. B., and Cirillo, A. C., Jr., *J. Vac. Sci. Technol.* **9,** 1073 (1972).
26. Clarkson, R. B., and Cirillo, A. C., Jr., *J. Catal.* **33,** 392 (1974).
27. Clarkson, R. B., and McClellan, S., *J. Phys. Chem.* **82,** 294 (1978).
28. Hermerschmidt, D., and Haul, R., *Ber. Bunsenges. Phys. Chem.* **85,** 739 (1981).
29. Tanaka, S., and Yamashina, T., *J. Catal.* **40,** 140 (1975).
30. Kubo, R., *J. Phys. Soc. Jpn.* **17,** 975 (1962).
31. Kittel, C., "Introduction to Solid State Physics." 3rd ed., Wiley, New York, 1966.
32. Dyson, F. J., *Phys. Rev.* **98,** 349 (1955).
33. Feher, G., and Kip, A. F., *Phys. Rev.* **98,** 337 (1955).
34. Griswold, T. W., Kip, A. F., and Kittel, C., *Phys. Rev.* **88,** 951 (1952).
35. Schultz, S., Shanabarger, M. R., and Platzman, P. M., *Phys. Rev. Lett.* **19,** 749 (1967).
36. Nishida, A., and Horai, K., *J. Phys. Soc. Jpn.* **59,** 3720 (1990).
37. Elliott, R. J., *Phys. Rev.* **96,** 266 (1954).
38. Anderson, K. L., Plischke, J. K., and Vannice, M. A., *J. Catal.* **128,** 148 (1991).
39. Seyedmonir, S. R., Strohmayer, D. E., Geoffroy, G. L., and Vannice, M. A., *Adsorpt. Sci. Technol.* **1,** 253 (1984).
40. Grant, R. B., Horbach, C. A. J., Lambert, R. M., and Tan, S. A., *J. Chem. Soc., Faraday Trans. 1* **83,** 2035 (1987).
41. Campbell, C. T., and Paffet, M. T., *Appl. Surf. Sci.* **19,** 28 (1984).
42. Campbell, C. T., and Koel, B. E., *J. Catal.* **92,** 272 (1985).